

Torsional Behavior of High-Strength Concrete Deep Beams with Variable Dimensions

TAMIM A. SAMMAN and ADEL A. MESAWA
*Civil Engineering Dept., Faculty of Engineering,
King Abdulaziz University, and Royal Saudi Airforce,
Prince Abdullah Airbase, Jeddah, Saudi Arabia*

ABSTRACT. Sixteen high-strength plain concrete deep beams were tested under pure torsion. The variables were the span/depth and the depth/width ratios. Concrete strength of about 67 MPa (9700 psi), span/depth ratios varying from 1 to 4 and depth/width ratios ranging from 2 to 5 were used. Test results showed that high-strength plain concrete deep beams under torsion failed suddenly and violently along a smooth surface, and the inclinations of the failure surfaces were influenced by both span/depth and depth/width ratios. The torsional capacity gradually increased as the span/depth ratio decreased from 3 to 1. The increase of span/depth or depth/width ratio reduced the beam stiffness and increased the angle of twist and the energy absorbed. The torsional strength of the test beams were also predicted using some of the theoretical equations available in the literature and were compared with the experimental values.

1. Introduction

Over the last decade, the application of high-strength concrete, *i.e.*, concrete with compressive strength in excess of 41 MPa (6,000 psi), has gained wide acceptance in construction industry and is currently being used in many parts of the world. Recent developments in material technology and the apparent advantages of high-strength concrete have encouraged engineers to produce and use concrete of high strength. However, adequate investigations on the aspects of its behavior in structural members are yet to be done. Therefore, a sufficient research data in this area is lacking. The ACI Committee 318^[1] has formulated design recommendations for normal-strength concrete shallow beams under both pure torsion and torsion with combined loading conditions. Engineers rely on these guidelines for the torsion design of deep

beams, *i.e.*, members with span/depth ratio of less than five, for both normal and high-strength concrete, without consideration to the differences in the behavior of deep and shallow beams under torsion^[2] and also between the characteristics of normal and high-strength concrete^[3,4]. The ACI Committee 363^[5] has urged for investigation of the various aspects of structural behavior of high-strength concrete members. To the authors' knowledge, only a single investigation on the behavior of high-strength concrete shallow members under torsion is reported so far^[6], and no work appears to be carried out on the torsional behavior of deep beams using high-strength concrete^[5,7]. Therefore, the objective of this investigation is to study the torsional behavior of high-strength concrete deep beams under torsion.

2. Prediction of Torsional Strength

The behavior of reinforced concrete beam in torsion before the onset of cracking, can be based on the study of plain concrete beam, because the contribution of reinforcement at this stage is negligible^[8]. Three theories, namely, elastic, plastic, and skew-bending theories^[8-12] have been developed to predict the torsional strength of plain concrete shallow members with rectangular cross sections. Recently, modifications to the skew-bending equation were proposed to predict the torsional capacities of high-strength plain concrete shallow beams^[6] and of normal-strength plain concrete deep beams^[2]. A brief review of these theories is now given.

2.1 Elastic Theory

The determination of the stress in non-circular members subjected to torsional loading is not as simple as that for circular section^[10]. However, results obtained from the theory of elasticity indicate that the torsional failure of a plain concrete member with rectangular cross section takes place when the maximum principal tensile stress, σ_{max} , becomes equal to the tensile strength of concrete, f'_t ^[11]. Since σ_{max} is equal to τ_{max} in pure shear, the elastic failure torque, T_e , can be estimated as

$$T_e = K_1 X^2 Y f'_t \quad (1)$$

where,

K_1 = St. Venant's coefficient, which depends on the aspect ratio, Y/X , of the member and varies from 0.208 to 0.333.

X, Y = The shorter and longer sides of the rectangular sections, respectively, mm or in.

f'_t = The tensile strength of concrete, $0.42 \sqrt{f'_c}$ (MPa) or $5 \sqrt{f'_c}$ (psi) as suggested by Hsu^[9].

The elastic theory was first used by Bach and Graf in 1912 and was widely adopted later by several investigators in this field^[10]. However, tests have shown that this theory consistently underestimates the failure strengths of plain concrete beams so that the test results obtained are roughly 50 percent greater than the predicted values^[9].

2.2 Plastic Theory

Nylander suggested that the extra strength that can not be achieved by the elastic theory may be contributed by the plastic properties of concrete^[9]. In other words, concrete may develop plasticity and thus increase the ultimate strength. Similar to elastic theory, failure is assumed to occur when the maximum principal tensile stress, σ_{max} , reaches the tensile strength of concrete, f'_t . The plastic failure torque, T_p , can therefore be evaluated as

$$T_p = K_2 X^2 Y f'_t \quad (2)$$

where

$K_2 = (0.5 - X/6Y)$, is the plastic coefficient which depends on Y/X and varies from 0.333 to 0.5

The plastic theory can roughly account for the extra strength that can not be explained by the elastic theory, because the coefficient K_2 is about 50 percent greater than K_1 used in the elastic theory. However, the plastic theory was found unsatisfactory^[9] because concrete is not ductile enough, particularly in tension to permit a perfect plastic distribution of shear. Therefore, the nominal torsional strength of a plain concrete section is somewhat between the values predicted by the elastic and plastic theories.

2.3 Skew-Bending Theory

This theory considers in detail the internal deformation behavior of a series of transverse warped surfaces along the beam. Initially presented by Lessig in 1958, it had subsequent contributions from several researchers in this field^[8]. Studies by Hsu^[9] have led to the conclusion that failure of a rectangular section in torsion occurs by bending about an axis parallel to the wider face of the section, and inclined at about 45° to the longitudinal axis of the beam. Based on this approach, the torsional strength, T_n , can be expressed as follows

$$T_n = \frac{X^2 Y}{3} (0.85 f_r) \quad (3)$$

where,

f_r = Modulus of rupture of concrete, MPa or psi.

The difference among the elastic, plastic and skew-bending theories lies only in the nondimensional coefficient and in the material constants. The coefficients K_1 and K_2 used in the elastic and plastic theories, respectively, are functions of Y/X , while the coefficient in the skew-bending theory is a constant ($=1/3$) and always lies between K_1 and K_2 . In the elastic and plastic theories, the material constant is the direct tensile strength of concrete, f'_t , while in the skew-bending theory, it is the modulus of rupture, $0.85 f_r$. Although f_r represents a type of indirect tensile strength, it is affected by the tensile strain gradient and, therefore, the size of the specimen.

Since the modulus of rupture is not often available for analysis and design, Hsu^[9] developed the following empirical equation to predict the nominal torsional capacity

of plain concrete beams, T_n , in terms of the concrete compressive strength

$$T_n = 6 (X^2 + 10) Y \sqrt[3]{f'_c} \quad (\text{psi units}) \quad (4)$$

where,

f'_c = Compressive strength of concrete, psi, and $x \geq 4$ in.

Bakhsh *et al.*^[6] showed experimentally that a better prediction of the nominal torsional capacity, T_n , of high-strength plain concrete shallow beams can be obtained by using the splitting tensile strength of concrete, f'_{sp} , in the skew-bending equation (Eq. 3) in lieu of $0.85 f'_c$, *i.e.*,

$$T_n = \frac{X^2 Y}{3} f'_{sp} \quad (5)$$

where,

f'_{sp} = Splitting tensile strength of concrete, MPa or psi.

2.4 Modified Skew-Bending Equation

for Normal-Strength Concrete Deep Beams

Akhtaruzzaman and Hasnat^[2] observed that the torsional strength of deep beams without a transverse opening remains practically constant for span/depth (L / Y) ratio ≥ 3.0 and increases with the decrease of L/Y ratio < 3.0 . They concluded that, as a lower-bound approach, the nominal torsional capacity, T_n , of normal strength plain concrete deep beams with solid cross section can be adequately evaluated by the following equations

$$T_n = 1.1 T_L \quad \text{for } L/Y \geq 3.0 \quad (6)$$

$$T_n = T_L (1.34 - 0.08 L/Y) \quad \text{for } L/Y < 3.0 \quad (7)$$

where,

$$T_L = \frac{0.85 X^2 Y}{3} f'_{sp}$$

L = Center-to-center span, mm. or in, and

L/Y = Span/depth ratio.

2.5 ACI Torsional Design Provisions

The ACI Code 318-89^[1] does not contain any design provision for deep beams under torsion. However, the present ACI procedure for the torsional design of normal strength shallow beams is based on the skew-bending theory and the recommendations of ACI Committee 438^[12]. Therefore, the nominal torsional strength, T_n , provided by concrete is specified to be as

$$T_n = \frac{X^2 Y}{3} (0.2 \sqrt{f'_c}) \quad (\text{S.I. units}) \quad (8)$$

$$T_n = \frac{X^2 Y}{3} (2.4 \sqrt{f'_c}) \quad (\text{psi units}) \quad (9)$$

3. Experimental Program

Sixteen beams were tested in this study. The dimensions of test specimens and the test variables are given in Table 1. The beams were divided into four groups on the basis of their Y/X and L/Y ratios. The beams are identified by one letter and two numbers. The letter "B" designates a beam, the first number indicates its Y/X ratio, and the second number represents its L/Y ratio. One concrete strength of about 67 MPa (9,700 psi) was used. The L/Y ratio was varied from 1 to 4, while the Y/X was varied from 2 to 5 to study their effect on the torsional capacity of deep beams. All beams had a constant depth of 400 mm, and the beam widths and spans were varied to achieve the desired L/Y and Y/X ratios.

TABLE 1. Test variables and experimental and theoretical torsional strength.

Group no.	Beam no.	Test variables					f'_c MPa	f'_{sp} MPa	f_t MPa	Theoretical torsional strength*								Exp. torque T_{exp} kN · N	$\frac{T_{exp}^{**}}{T_{th}}$
		Span L m	X mm	Y mm	Y/X	L/Y				Eq. 1 kN-m	Eq. 2 kN-m	Eq. 3 kN-m	Eq. 4 kN-m	Eq. 5 kN-m	Eq. 6,7 kN-m	Eq. 8 kN-m			
(1)	(2)	(3)	(4)	(5)	(6)	(7)	(8)	(9)	(10)	(11)	(12)	(13)	(14)	(15)	(16)	(17)	(18)	(19)	
1	B 21	0.4	200	400	2	1	66.91	5.30	6.42	13.52	22.91	29.10	16.46	28.27	30.27	8.93	30.12	0.99	
	B 22	0.8	200	400	2	2	66.91	5.30	6.42	13.52	22.91	29.10	16.46	28.27	28.35	8.93	25.90	0.91	
	B 23	1.2	200	400	2	3	66.91	5.30	6.42	13.52	22.91	29.10	16.46	28.27	26.43	8.93	23.90	0.90	
	B 24	1.6	200	400	2	4	66.91	5.30	6.42	13.52	22.91	29.10	16.46	28.27	26.43	8.93	24.47	0.93	
2	B 31	0.4	135	400	3	1	66.91	5.30	6.42	6.69	11.12	13.26	8.75	12.88	13.79	3.98	13.85	1.00	
	B 32	0.8	135	400	3	2	66.91	5.30	6.42	6.69	11.12	13.26	8.75	12.88	12.92	3.98	12.75	0.99	
	B 33	1.2	135	400	3	3	66.91	5.30	6.42	6.69	11.12	13.26	8.75	12.88	12.04	3.98	10.90	0.90	
	B 34	1.6	135	400	3	4	66.91	5.30	6.42	6.69	11.12	13.26	8.75	12.88	12.04	3.98	11.00	0.91	
3	B 41	0.4	100	400	4	1	66.91	5.30	6.42	3.94	6.30	7.28	5.80	7.01	7.57	2.18	7.20	0.95	
	B 42	0.8	100	400	4	2	66.91	5.30	6.42	3.94	6.30	7.28	5.80	7.01	7.10	2.18	6.37	0.90	
	B 43	1.2	100	400	4	3	66.91	5.30	6.42	3.94	6.30	7.28	5.80	7.01	6.61	2.18	6.14	0.93	
	B 24	1.6	100	400	4	4	66.91	5.30	6.42	3.94	6.30	7.28	5.80	7.01	6.61	2.18	5.99	0.91	
4	B 51	0.4	80	400	5	1	66.91	5.30	6.42	2.55	4.11	4.66	3.73	4.52	4.84	1.40	4.70	0.97	
	B 52	0.8	80	400	5	2	66.91	5.30	6.42	2.55	4.11	4.66	3.73	4.52	4.54	1.40	4.50	0.99	
	B 53	1.2	80	400	5	3	66.91	5.30	6.42	2.55	4.11	4.66	3.73	4.52	4.00	1.40	3.90	0.98	
	B 54	1.6	80	400	5	4	66.91	5.30	6.42	2.55	4.11	4.66	3.73	4.52	4.00	1.40	4.10	1.03	

*For all beams, average material properties are used.

** T_{th} is calculated from the applicable Eq. 6 or 7.

A general purpose ordinary portland cement (Type I) was used in this experimental work. Sand with high fineness modulus of (3.1), and coarse aggregates with a maximum size of 10 mm (3/8 in.) were employed. A dark gray densified silica fume with a specific gravity of 2.2 (compared to that of 3.1 for ordinary portland cement) was used. The bulk density of the silica fume was around 6.00 kN/m³ (37.6 lb/ft³). A

super-plasticizer was used to lower the water requirement of the concrete mix, to provide good workability and to increase strength by virtue of lowering the water/cement ratio. Table 2 shows the mix proportions and mechanical properties of concrete used.

TABLE 2. Details of mix and mechanical properties of concrete.

Group no.	Mix proportion* (by weight) C: F. A: C. A	W/C ratio	Plasticizer %	Silica fume %	Slump (mm)	Compressive strength** (f'_c) MPa		Splitting** tensile strength (f'_{sp}) MPA	Modulus of rupture (f'_r) MPA
						(7)	(7)		
(1)	(2)	(3)	(4)	(5)	(6)	on the day of testing	At 28 days	(8)	(9)
1	1:1.2:1.8	0.27	6	0	70	66.21 (28 days)	66.21	5.24	6.27
2	1:1.2:1.8	0.27	6	0	65	68.23 (28 days)	68.23	5.40	6.37
3	1:1.8:1.20	0.27	6	0	98	66.91 (28 days)	66.91	5.30	6.42
4	1:1.4:1.1	0.21	6	10	60	67.75 (14 days)	89.70	5.36	6.51
Average material properties for all groups					65	66.91	70.81	5.30	6.42

*C = Cement, F.A. = Fine aggregate, C.A. = Coarse aggregate.

**Average value of three specimens.

Concrete was placed in three layers in the formwork and internally consolidated with an electrical vibrator to produce uniform concrete without any segregation. For each group of beams, eight 150×300 mm (6×12 in.) cylinders and four $150 \times 150 \times 510$ ($6 \times 6 \times 17$ in.) prisms were cast. Curing of beams and control specimens was done by watering them once daily and keeping them covered with a plastic sheet until 24 hours before testing to prevent the loss of moisture. All beams and control specimens were cured in the same room and under similar conditions. Before testing, the beams were coated with a white paint to facilitate the observation of cracking patterns.

The beams were tested under the action of pure torsion. Special bearings at the supports insured that the test beam was free to twist at one end while the other end was held against torsional rotation as shown in Fig. 1. The load was applied in small increments up to failure. At the end of each load increment, torsional rotations of the beam at both ends, and crack development and propagation on the beam surfaces were recorded. The failure-crack inclinations were also measured at the end of the test.

4. Test Results and Discussion

The test results are analysed and compared to existing theories as follow :

4.1 Experimental Torsional Strength

The effect of L/Y ratio on the experimental torsional strength, T_{exp} , of the tested beams are shown in Table 1 and Fig. 2. For beams with constant Y/X ratio, the tor-

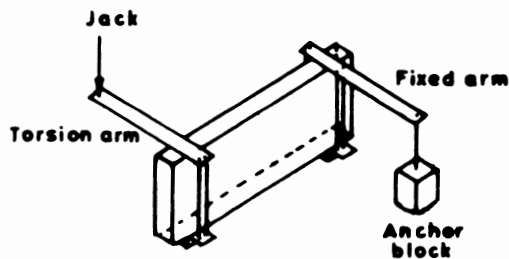
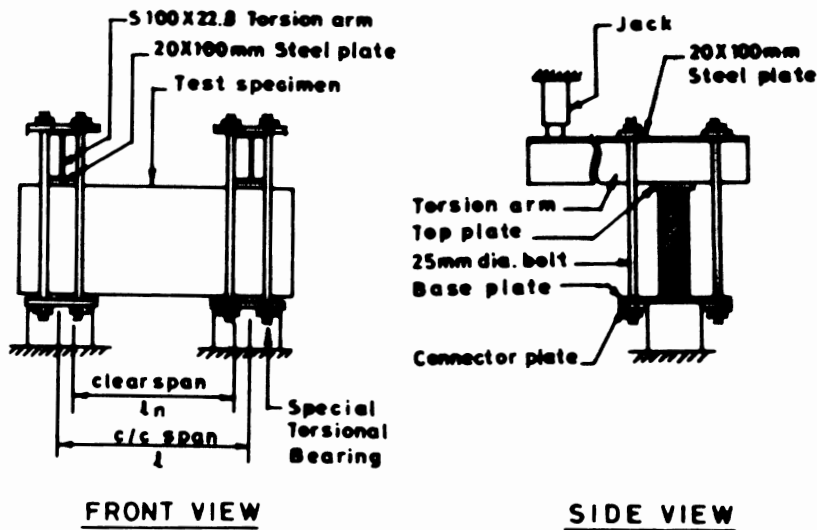


FIG. 1. Test set-up.

sional strength is approximately constant for $L/Y \geq 3.0$ and gradually increases for $L/Y < 3.0$. This observation is similar to the one reported by Akhtaruzzaman and Hasnat^[2]. The increase in the torsional strength in the region of $L/Y < 3.0$ may be explained by the fact that the torsional load and the clamping reactions at the supports are distributed over larger length, thereby enlarging concrete confinement zone. Figure 3 shows that when the L/Y ratio is large, the confinement zones are located near the supports. However, when the L/Y ratio is small, the confining zones may overlap and the beam is subjected to compressive stresses in addition to the torsional shearing stresses. The test results show that decreasing the L/Y ratio from 3 to 1 or Y/X ratio from 5 to 2 increases the torsional strength from 3.90 kN · m to 30.12 kN · m depending on the Y/X and L/Y ratios.

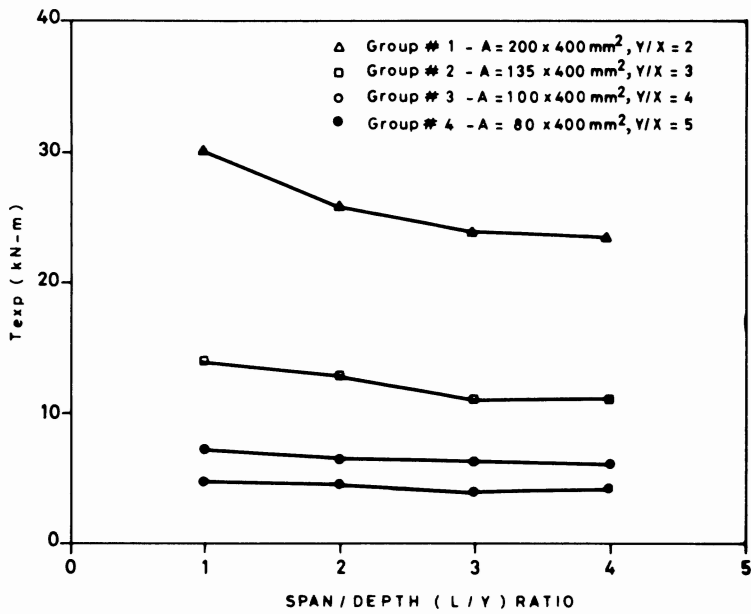


FIG. 2. Effect of span/depth (L/Y) ratio on the experimental torsional strength.

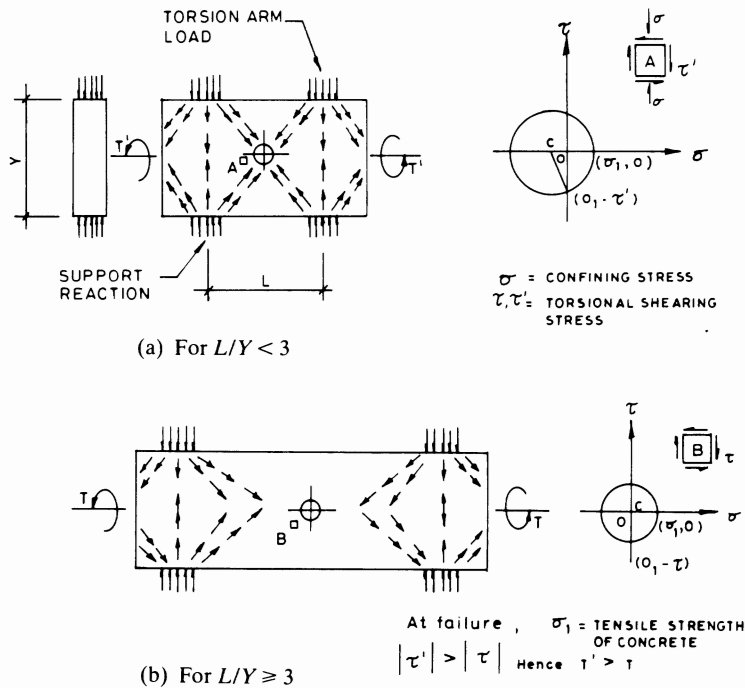


FIG. 3. Load dispersion and Mohr's stress circles (Ref. 2)

4.2 Crack Pattern and Failure Mode

In all the beams, no crack was observed during the test prior to failure. When the failure loads were reached, the beams failed suddenly and violently along smooth inclined surfaces. The failure-crack inclinations with respect to the beam axis were different on the two vertical sides of the beams. Figure 4 shows the failure-crack patterns of some of the test beams. Only one mode of failure, *viz.*, shear failure was observed.

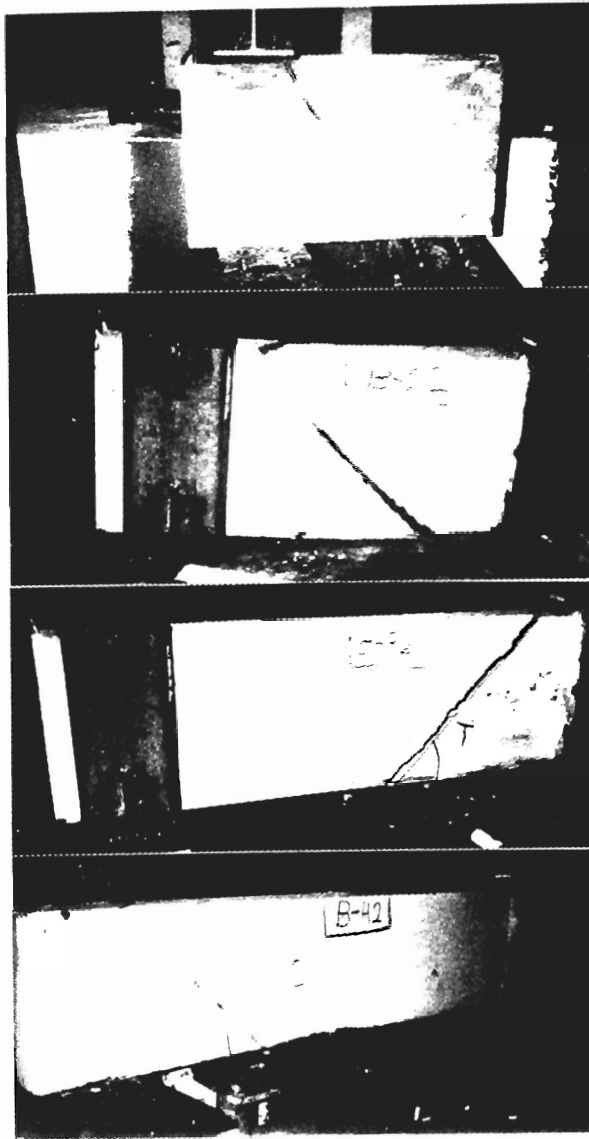


FIG. 4. Typical crack patterns.

Table 3 presents the failure-crack inclination angles on the two vertical faces (tension and compression failure inclination angles) of the beams of different groups. The inclinations were evaluated by choosing the best fit straight line along the cracked surface. Figures 5 and 6 show the failure inclination angles plotted as a function of the L/Y ratios for the tension and the compression cracks, respectively, on the two vertical faces of the tested beams. The inclinations of the tension failure cracks varied from 36.71 to 69.26 degrees depending on the Y/X and L/Y ratios. This indicates that a modification to the skew-bending theory is needed to predict the torsional strength of high-strength concrete deep beams, since it assumes a 45° failure plane. The inclination is found to increase with the decrease of L/Y ratio from 3 to 1. This is similar to the effect of L/Y ratio on the torsional capacity for the test beams. The inclination of a compression crack was always found lower than that of the corresponding tension crack and varied from 30.30 to 63.10 degrees depending upon the Y/X and L/Y ratios.

4.3 Theoretical Torsional Strengths

The theoretical torsional strengths, T_{th} , of the test beams were estimated using the following methods :

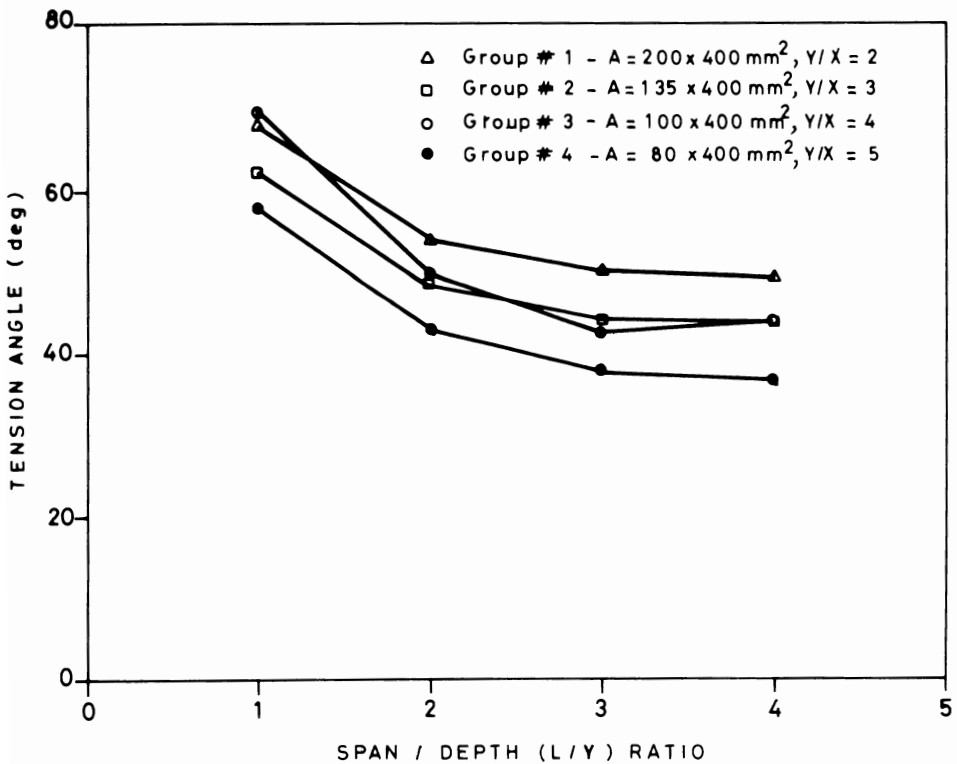


FIG. 5. Effect of span/depth (L/Y) ratio on the tension crack angle.

1. Elastic theory (Eq. 1).
2. Plastic theory (Eq. 2).
3. Skew-bending theory in terms of the modulus of rupture (Eq. 3).
4. Skew-bending theory in terms of the compressive strength (Eq. 4).
5. Skew-bending theory in terms of the splitting tensile strength (Eq. 5).

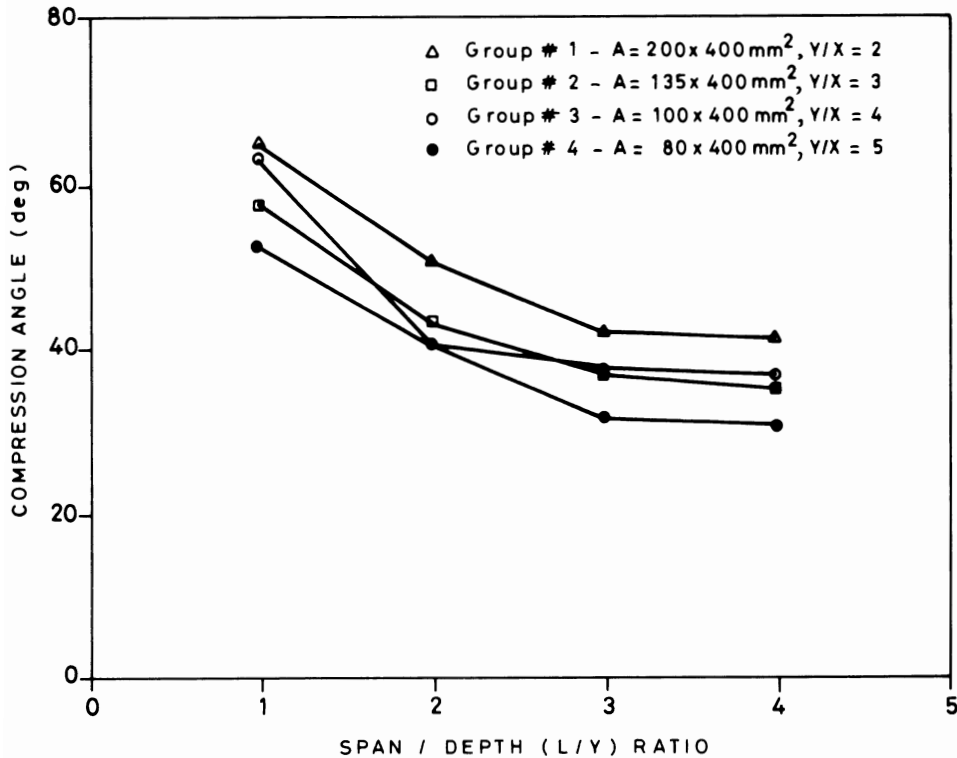


FIG. 6. Effect of span/depth (L/Y) ratio on the compression crack angle.

TABLE 3. Inclination of tension and compression failure-cracks for the tested beams.

Span/depth (L/Y) ratio	Inclination of tension cracks (degrees)				Inclination of compression cracks (degrees)			
	Group # 1	Group # 2	Group # 3	Group # 4	Group # 1	Group # 2	Group # 3	Group # 4
	$Y/X = 2$	$Y/X = 3$	$Y/X = 4$	$Y/X = 5$	$Y/X = 2$	$Y/X = 3$	$Y/X = 4$	$Y/X = 5$
1	67.61	62.01	69.26	57.37	57.75	57.75	63.10	52.55
2	53.83	48.35	49.90	42.57	50.54	43.10	40.54	37.10
3	50.42	44.79	42.45	37.59	42.0	36.64	37.19	31.57
4	49.63	43.79	43.79	36.71	41.02	34.92	36.57	30.30

6. The equations proposed by Akhtaruzzaman and Hasnat^[2] for deep beams (Eq. 6, 7).
7. ACI Code equation (Eq. 8).

The experimental torsional strengths of the test beams and their theoretical strengths are computed and presented in Table 1 and in Fig. 7 through 10. Table 1 shows that the elastic and the plastic theories, and the skew-bending theory in terms of the compressive strength, and the ACI Code 318-89 equation are always conservative in predicting the torsional strengths of the test beams by 52 to 123%, 1 to 31%, 3 to 83% and 174 to 248%, respectively. The skew-bending theory in terms of the splitting tensile strength and the modulus of rupture overestimates the torsional strengths of the test beams by 0.4 to 18% and 1 to 22%, respectively. Figures 7 to 10 show that, the theoretical torsional strength computed on the basis of Akhtaruzzaman and Hasnat^[2] equations (Eq. 6 and 7) gives the best prediction for the experimental torsional strength (T_{exp}/T_{th} values close to 1.0). It is found that the main parameters which affect the torsional strength are the splitting tensile strength, f'_{sp} , L/Y , and Y/X ratios.

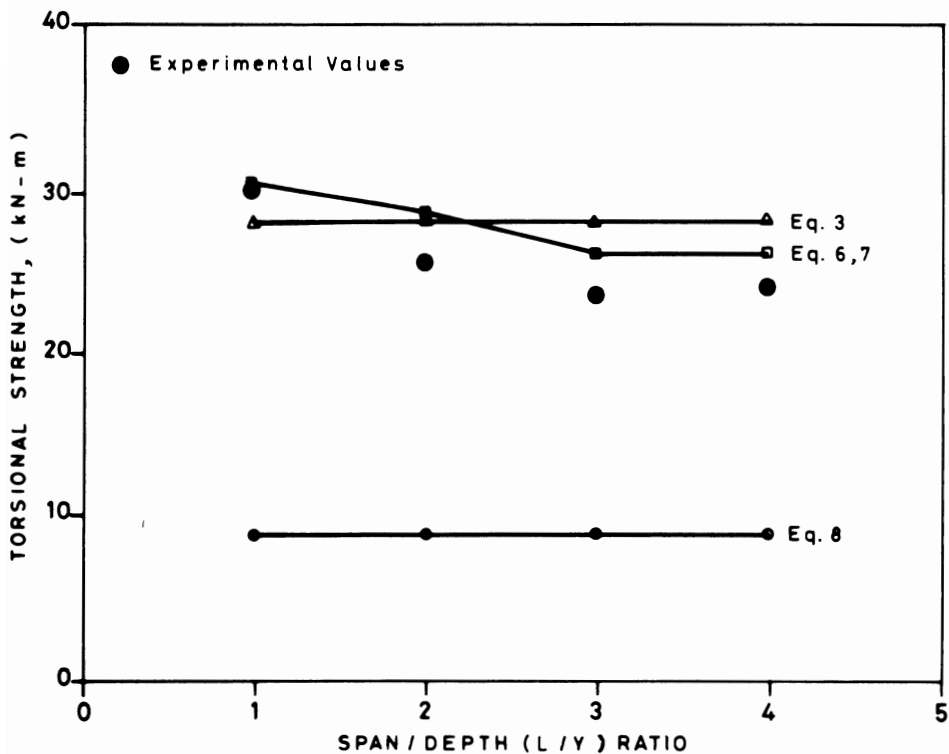


FIG. 7. Effect of span/depth (L/Y) ratio on the experimental and the theoretical torsional strength for beams of group # 1 ($Y/X = 2$).

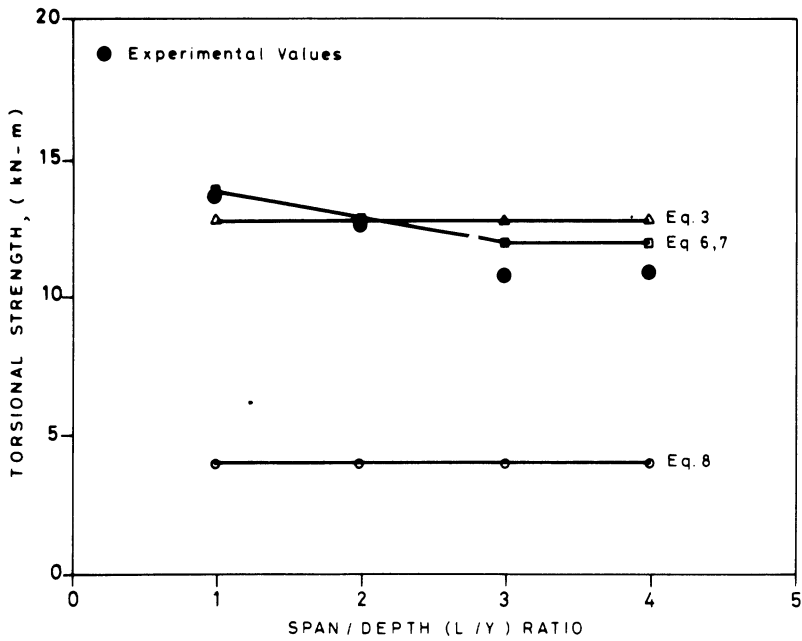


FIG. 8. Effect of span/depth (L/Y) ratio on the experimental and the theoretical torsional strength for beams of group # 2 ($Y/X = 3$).

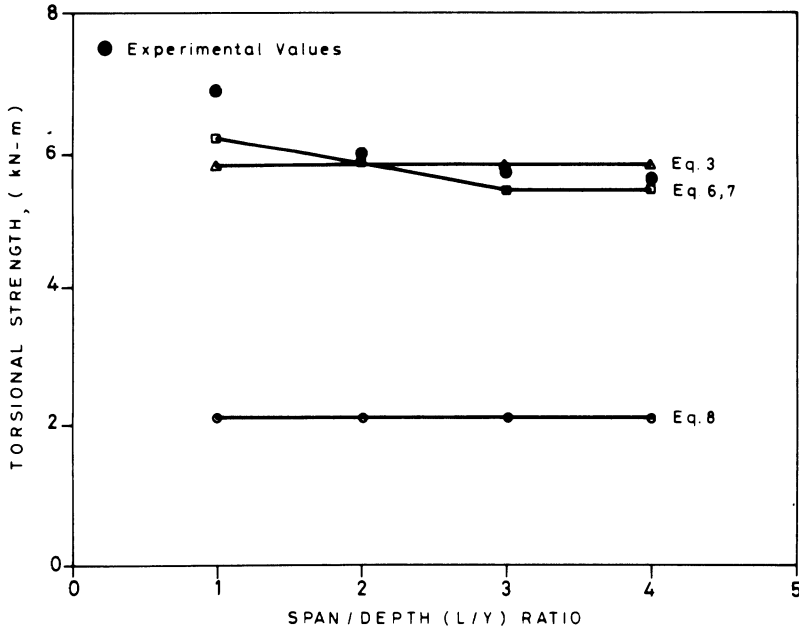


FIG. 9. Effect of span/depth (L/Y) ratio on the experimental and the theoretical torsional strength for beams of group # 3 ($Y/X = 4$).

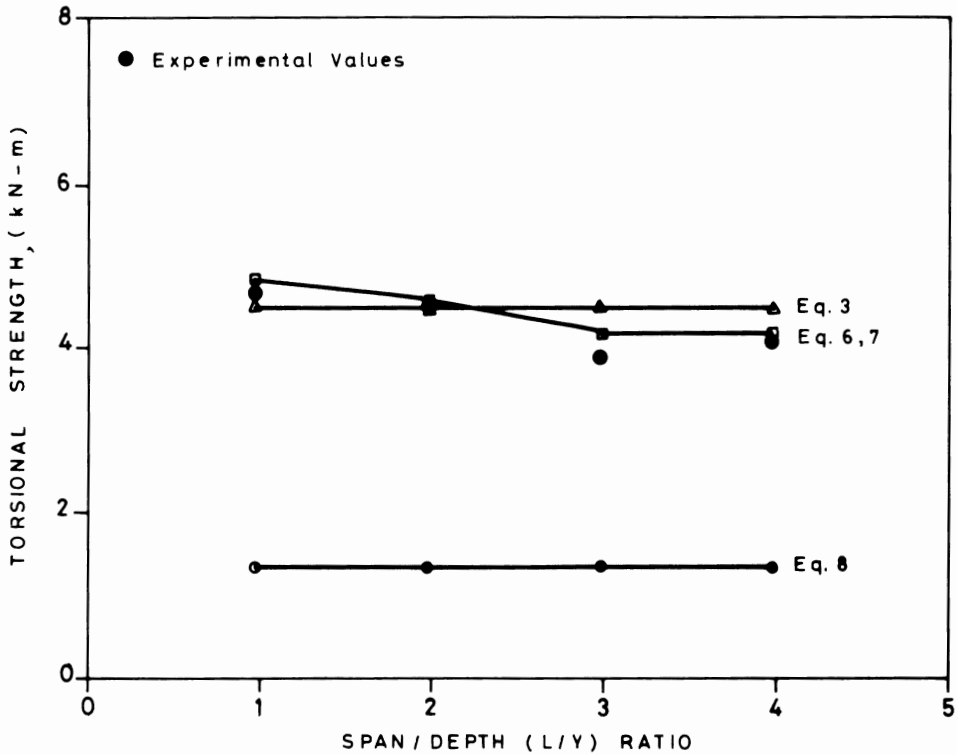


FIG. 10. Effect of span/depth (L/Y) ratio on the experimental and the theoretical torsional strength for beams of group # 4 ($Y/X = 5$).

4.4 Twisting Characteristics

Figure 11 shows the torque-twist relationship of the test beams. The torque-twist curves are approximately linear up to 50% of the respective torsional strength; thereafter the curves become non-linear and the torsional stiffness is reduced in this range, as could be noticed from the reduced slopes of the curves. Figure 11 shows that the angle of twist, θ , increases with the increase of L/Y or Y/X ratio provided that all other variables are constant. The energy absorbed as estimated as the area under the torque-twist curve increases with the increase of L/Y or Y/X ratio.

Conclusion

Based on the test results of sixteen high-strength plain concrete deep beams tested under pure torsion, the following conclusions can be drawn :

1. For beams with constant depth/width (Y/X) ratio, torsional strength of high-strength plain concrete deep beams gradually increases as the span/depth (L/Y) ratio decreases from 3 to 1.
2. In all the beams, no crack was observed during the testing prior to failure. When the failure load was reached, the beams failed suddenly and violently along

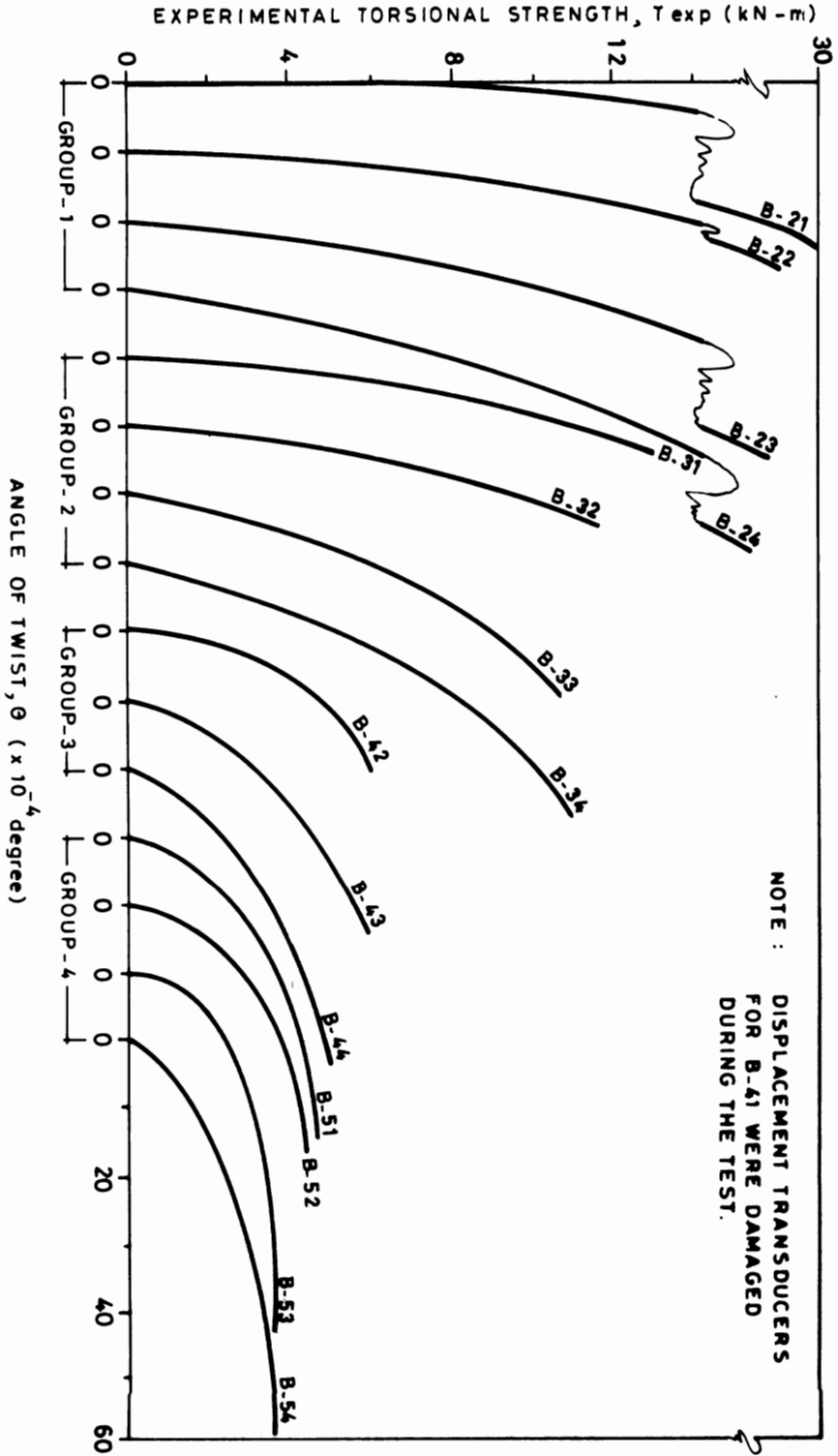


FIG. 11. Torque-twist relationship.

smooth inclined surfaces.

3. The failure-crack inclinations on the beam surfaces were influenced by span/depth and depth/width ratios.

4. Akhtaruzzaman and Hasnat equation^[2] gives the closest predictions of the experimental torsional strength.

5. The main parameters which affect the torsional strength are the splitting tensile strength, f'_{sp} , span/depth, and depth/width ratios.

6. The angle of twist, θ , for the test beams increases with the increase of span/depth or depth/width ratio. This indicates that the energy absorbed by the beams increases with the increase of L/Y ratio or Y/X ratio.

7. The ACI 318-89 Code torsional equation for normal strength shallow beams is highly conservative by 174 to 248% in predicting the torsional strengths of the high-strength plain concrete deep beams tested in this study.

References

- [1] ACI (American Concrete Institute) Committee 318, *Building Code Requirements for Reinforced Concrete (ACI 318-89)*, Detroit, 353 p. (1989).
- [2] Akhtaruzzaman, A.A. and Hasanat, A., Torsion in deep beams with an opening, *ACI Structural Journal*, **86**(1): 20-25 (1989).
- [3] Khaloo, R. and Ahmed, S.H., Behavior of high-strength concrete under torsional triaxial compression, *ACI Materials Journal, Proceedings*, **86**(6): 550-558 (1989).
- [4] Slate, O.F., Nilson, A.H. and Martinez, S., Mechanical properties of high-strength light weight concrete, *ACI Journal, Proceedings*, **83**(4): 606-613 (1986).
- [5] ACI Committee 363, Research needs for high-strength concrete (ACI 363-IR-87), *ACI Materials Journal, Proceedings* **84**(6): 559-561 (1987).
- [6] Bakhsh, H., Wafa, F. and Akhtaruzzaman, A., Torsional behavior of plain high-strength concrete beams, *ACI Structural Journal, Proceedings*, **87**(5): 587-588 (1990).
- [7] ACI Committee 363, State-of-the-art-report on high-strength concrete, *ACI Journal, Proceedings*, **81**(4): 365-387 (1984).
- [8] Nawy, G.E., *Reinforced Concrete*, Prentice-Hold Inc., Englewood Cliffs, New Jersey, 227 p. (1985).
- [9] Hsu, T.T.C., *Torsional Reinforced Concrete*, Van Nostrand Reinhold Company, New York, 516 p. (1984).
- [10] Hassoun, M.N., *Design of Reinforced Concrete Structure*, PWS Publisher, Boston, Massachusetts, 470 p. (1985).
- [11] Hsu, T.T.C., *Torsion of Structural Plain Concrete Rectangular Sections*, Torsion of Structural Concrete, ACI Special Publ. SP-18, pp. 203-238 (1968).
- [12] ACI Committee 438, Tentative recommendations for the design of reinforced concrete members to resist torsion, *ACI Journal, Proceedings*, **66**(1): 576-588 (1969).

السلوك الالتوائي للكمرات العميقة المصنعة من الخرسانة عالية المقاومة ذات أبعاد متغيرة

تميم عبد الهادي سمان و عادل أحمد مساوي

قسم الهندسة المدنية ، كلية الهندسة - جامعة الملك عبدالعزيز
والقوات الجوية الملكية السعودية ، قاعدة الأمير عبدالله الجوية ،
جدة ، المملكة العربية السعودية

المستخلص . أختيرت ست عشرة كمرّة عميقة مصنعة من الخرسانة عالية المقاومة تحت تأثير الالتواء . كانت المتغيرات ؛ نسب الطول إلى العمق والعمق إلى العرض . تم استخدام خرسانة بقوة ٦٦,٩١ ميجاباسكال ، ونسب الطول إلى العمق متغيرة من ١ إلى ٤ ، ونسب العمق إلى العرض متراوحة من ٢ إلى ٥ . انكسرت الكمرات العميقة المصنعة من الخرسانة عالية القوة تحت تأثير الالتواء بشكل مفاجئ محدثة صوتًا مرتفعًا ، وكان سطح الكسر ناعمًا . زوايا ميل أسطح الانكسارات تأثرت بنسب الطول إلى العمق والعمق إلى العرض معًا . مقاومة الالتواء تزداد تدريجيًا كلما نقصت نسبة الطول إلى العمق من ٣ إلى ١ . الزيادة في نسبة الطول إلى العمق أو العمق إلى العرض تقلل من صلابة الكمرّة وتزيد زاوية الالتواء والطاقة الممتصة . تم حساب قوة الالتواء للكمرات المختبرة باستخدام بعض المعادلات النظرية المتوافرة في المراجع ، ومن ثم مقارنتها بقيم التجارب .